

## $\Lambda$ -Nuclear Properties from the Spectroscopy of ${}^{13}_{\Lambda}\text{C}$

E. H. Auerbach, A. J. Baltz, C. B. Dover, A. Gal,<sup>(a)</sup> S. H. Kahana,  
L. Ludeking,<sup>(b)</sup> and D. J. Millener

*Brookhaven National Laboratory, Upton, New York 11973*

(Received 29 June 1981)

A comprehensive shell model for light hypernuclei has been developed and applied to  ${}^{13}_{\Lambda}\text{C}$ . Absolutely normalized distorted-wave calculations yield angular distributions in excellent agreement with experiment, allowing spin assignments to be made. Coherences arising from the distinguishability of the  $\Lambda$  are predicted theoretically and observed in the data. The overall comparison with experiment places constraints on residual interaction matrix elements.

PACS numbers: 21.80.+a, 25.80.+f

The preceding Letter<sup>1</sup> reports on spectra measured for several  $p$ -shell hypernuclei produced via the  $(K^-, \pi^-)$  reaction at 800 MeV/ $c$ . In particular the rich spectrum generated for  ${}^{13}_{\Lambda}\text{C}$  provides a fertile ground for a sophisticated shell model treatment of hypernuclei. We have developed a formalism appropriate to  $(p_N)^n p_{\Lambda}$  configurations so as to naturally account for the  $(0p_N^{-1}, 0p_{\Lambda})$  excitations which appear to dominate the hypernuclear spectra obtained in Ref. 1. Augmenting this scheme by calculations of the  $(p_N)^n s_{\Lambda}$  configuration,<sup>2</sup> we are able to present a comprehensive picture of hypernuclear structure in this mass region. This formalism allows us to deal with the occasional, very revealing, departures from a simple weak-coupling picture. In particular, the excitation-strength ratio for the lowest two  $\frac{1}{2}^-$  substitutional states in  ${}^{13}_{\Lambda}\text{C}$  differs strongly from

a simple pickup value. Further, our approach permits us to extract constraints on the  $\Lambda$  spin-orbit forces from the energy shift with angle for a peak expected to arise from the  ${}^{12}\text{C}(\text{g.s.}) \otimes (p_{1/2}, p_{3/2})_{\Lambda}$  configurations. Coupled to our structure treatment is the use of a distorted-wave Born-approximation<sup>3</sup> reaction mechanism, incorporating a fit to preliminary elastic-scattering data,<sup>4</sup> which should yield an accurate determination of absolute cross sections.

The process being considered,

$$K^- + {}^A Z(i) \rightarrow \pi^- + {}^A_{\Lambda} Z(f), \quad (1)$$

is best treated in the laboratory system where it is reasonable to assume that the  $K^-$ -nucleus many-body amplitude is given by a sum over elementary two-body interactions. The differential cross section for (1) may be written

$$\left(\frac{d\sigma}{d\Omega_L}\right) = J \frac{\prod E_L}{\prod E} \frac{k'/k}{(2\pi\hbar^2 c^2)^2} \frac{\prod E}{(E_{\text{total}})^2} V_I^2 |\bar{T}_{if}|^2, \quad (2a)$$

$$\bar{T}_{if} = \int d^3r \chi_{\pi^-}^{(-)*}(\vec{r}) \langle {}^A Z(f) | \sum_j \delta(\vec{r} - \vec{r}_j) u^-(j) | {}^A Z(i) \rangle \chi_{K^-}^{(+)}(\vec{r}). \quad (2b)$$

$J$  is the c.m.-laboratory Jacobian,  $\prod E$  and  $\prod E_L$  are products of the energies for the four bodies involved in Eq. (1) in the center-of-mass and laboratory systems, respectively, and  $E_{\text{total}} = E_K + E_{AZ}$  (c.m.).  $V_I = 165 \text{ MeV fm}^3$  is a volume integral determined from the elementary two-body  $0^\circ$  laboratory cross section, taken<sup>5</sup> as 4.5 mb/sr but reduced to 3.2 mb/sr by an appropriate Fermi averaging in the nucleus. Potentials which fit available elastic data<sup>4</sup> on  ${}^{12}\text{C}$  are  $U_K(\vec{r}) = (-24.4 - i41.4)f(r, 0.375, 1.075)$  MeV, and  $U_{\pi}(\vec{r}) = (-0.9 - i50.9)f(r, 0.44, 0.926)$  MeV with  $f(r, a, r_0)$  the usual Woods-Saxon form for diffusivity  $a$  (fm) and radius  $R = r_0 A^{1/3}$  (fm). Small  $\langle r^2 \rangle$  for  $U_{K, \pi}$  reflect expected short ranges for  $\pi^-$ - and  $K^-$ -nucleon forces.

A final ingredient in the reaction calculation is the choice of  $\Lambda$  and neutron bound-state wave functions. The Woods-Saxon potentials for the bound states in masses 12 and 13 were chosen consistent with electron-scattering charge distributions and with single-particle energies for both neutrons and protons. The  $\Lambda$ -binding energies are somewhat arbitrary; in both masses 12 and 13 we took  $B_{\Lambda}(p_{3/2}, p_{1/2}) = (0.6, 0.1)$  MeV implying a small spin-orbit separation<sup>6</sup>  $\epsilon_p \equiv \epsilon_{p_{1/2}}(\Lambda) - \epsilon_{p_{3/2}}(\Lambda) = 0.5$  MeV. The geometry for  $\Lambda$  and nucleon potentials was identical,  $r_0 = 1.15$  fm,  $a = 0.63$  fm.

The effective neutron number  $|\bar{T}_{if}|^2$  in Eq. (2) contains a coherent superposition over neutron and  $\Lambda$  orbits  $j_{\Lambda}, j_N$ . Neglecting detailed dependences on  $j_N, j_{\Lambda}$  this quantity becomes proportional to

$$\langle l_N 0 k 0 | l_{\Lambda} 0 \rangle^2 (\alpha_f J_f T_f) \| (a_{i_{\Lambda}} \dagger \bar{a}_{i_N})^{\Delta L = k, \Delta S = 0} \| \alpha_i J_i T_i \rangle^2 M^{(k)}(\theta). \quad (3)$$

All structure information is contained in the transition density, calculable after consistent treatment of  ${}^A Z$  and  ${}^A \Lambda Z$ . For  $0p_N-0p_\Lambda$  transitions, the independent magnitudes  $M^{(0)}$ , which falls away rapidly from  $\theta_L=0^\circ$ , and  $M^{(2)}$ , which peaks near  $15^\circ$  in this situation (see Fig. 2), excite different final  ${}^{13}\text{C}$  states,  $\frac{1}{2}^-$  for  $k=0$  and  $\frac{3}{2}^-$ ,  $\frac{5}{2}^-$  for  $k=2$  corresponding to  $\Delta J=\Delta L=k$ . In the pure weak-coupling limit, the entire cross section associated with a single core state  $\{c\}$  is simply related to the neutron pickup strength,

$$|\tilde{T}_{if}|^2 = \sum_k (2k+1) \langle l_N 0 k 0 | l_\Lambda 0 \rangle^2 M^{(k)}(\theta) \sum_j C^2 S_j(c). \quad (4)$$

A poor-resolution ( $K^-, \pi^-$ ) experiment would see just this strength.

The structure calculations employ two versions for the  $p$ -shell effective interaction, one due to Cohen and Kurath<sup>7</sup> (POT) and one due to Millener (MP4), and in principle a completely general  $\Lambda N$  force. In practice we used central and two-body spin-orbit components (symmetric and antisymmetric):

$$V_{\Lambda N}(r) = -V(r)(1 - \epsilon + \epsilon P_x)(1 + \alpha \vec{\sigma}_N \cdot \vec{\sigma}_\Lambda) + v_\pm(r)(\vec{\sigma}_\Lambda \pm \vec{\sigma}_N) \cdot \vec{I}_{NA}. \quad (5)$$

The relevant Slater integrals of the central interaction are  $F^{(0)}$  and  $F^{(2)}$ . We take<sup>8</sup>  $F^{(0)} = -1.16$  MeV,  $\alpha = -0.1$ ,  $\epsilon = 0$  and calculate the  ${}^{13}\text{C}$  spectrum as a function of  $\epsilon_p$  and  $F^{(2)}$ . Since the lowest states of the  ${}^{12}\text{C}$  core have dominantly  $S=0$ , forces involving  $\vec{\sigma}_N$  play only a minor role in the structure of  ${}^{13}\text{C}$ . Sufficient core states are employed in our  $(p_N)^n p_\Lambda$  weak-coupling basis to guarantee convergence and this accounts for all pickup strength and all states of high spatial symmetry. Note that if we treat the hyperon as a distinguishable nucleon in a harmonic-oscillator basis then all  $s^4 p^n p_\Lambda$  configurations have an overlap of  $A^{-1/2}$  with spurious states. Since this overlap is small and uniform we consider  $s^4 p^n p_\Lambda$  configurations only.

Several interesting points emerge from the calculations. The comparison of absolutely normalized angular distributions with data in Fig. 1 indicates the striking success of the overall approach. Figure 2 presents the essence of the structure results, with detailed information available only from analysis of the "10"- and "16"-MeV groups (Ref. 1). Figure 3(a) displays energy splittings between different states as a function of  $F^{(2)}$ . At small angles the cross-section ratio  $r = \sigma((\frac{1}{2}^-)_2) / \sigma((\frac{1}{2}^-)_1)$ , like  $\Delta E((\frac{1}{2}^-)_2 - (\frac{1}{2}^-)_1)$ , is strongly dependent on  $F^{(2)}$ ; for MP4 (POT),  $\rho$

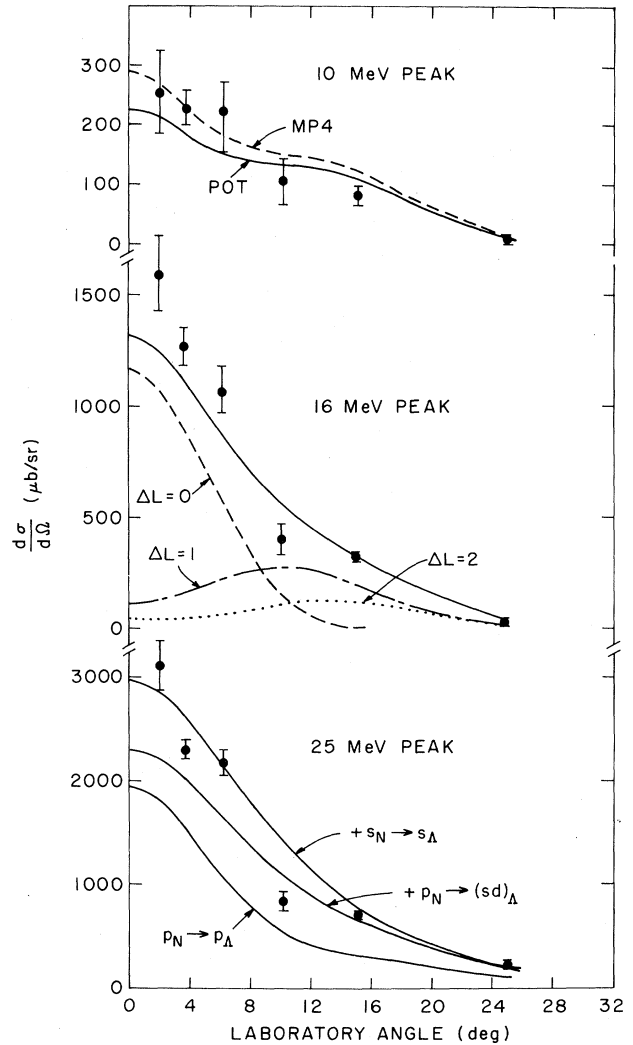


FIG. 1. Comparison of calculated angular distributions with experimental data (Ref. 1); the data points and curves represent cross sections summed over the same region of excitation energy. The demarcation between the 16- and 25-MeV peaks is changed from 20 to 18 MeV for angles greater than  $10^\circ$  in accordance with the data. The cross-section shapes for  $p_N \rightarrow p_\Lambda$   $\Delta L=0$  or 2 and  $p_N \rightarrow s_\Lambda$   $\Delta L=1$  [ $\Delta L=k$  in Eqs. (3) and (4)] are shown in the breakdown of the cross section for the 16-MeV peak. For the 25-MeV peak the incremental contributions from  $p_N \rightarrow p_\Lambda$  ( $\Delta L=0+2$ ),  $p_N \rightarrow (sd)_\Lambda$  ( $\Delta L=1+3$ ), and  $s_N \rightarrow s_\Lambda$  ( $\Delta L=0$ ) transitions are given. In the  $\Delta L=0$  contribution to the 10-MeV peak there is destructive interference between the  $j_N=j_\Lambda=\frac{1}{2}$  and  $j_N=j_\Lambda=\frac{3}{2}$  amplitudes. The cross section is thus small and sensitive to the model chosen for the core wave functions; cross sections are given for two interactions (see text) which fit the available data on  $p$ -shell nuclei well. An additional error of  $\pm 20\%$  in overall normalization assigned in Ref. 1 is not shown, and theoretical uncertainties are of this order.

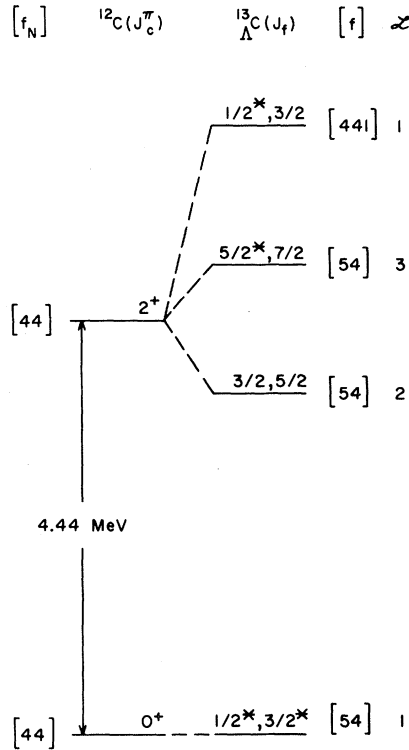


FIG. 2.  $^{12}\text{C}(0^+, 2^+) \otimes p_\Lambda$  spectrum for an interaction independent of  $\sigma_\Lambda$  [ $F^{(2)} = -3$  MeV,  $\epsilon = 0$ ]. States dominant in the 10- and 16-MeV peaks at  $0^\circ$  and  $15^\circ$  are marked with asterisks.  $\mathcal{L} = \vec{J}_c + \vec{I}_\Lambda$  is a good quantum number and the indicated degeneracies result, independent of the size of the nuclear core basis. The dominant spatial symmetry for each state is also given.

varies from 5.2 to 6.4 (7.3 to 9.3) as  $F^{(2)}$  ranges from  $-3.0$  to  $-3.6$  MeV. Despite the weak  $\Lambda N$  force, the lower state (for  $F^{(2)} = -3.0$ )

$$\psi\left(\left(\frac{1}{2}^-\right)_1\right) = 0.959|^{12}\text{C}(\text{g.s.}) \otimes p_{1/2}\rangle - 0.283|^{12}\text{C}(2^+) \otimes p_{3/2}\rangle$$

indicates a tendency by the hypernucleus to seek a good spatial symmetry [54], containing 0.88 of this latter configuration of amplitude and only  $-0.15$  for the substituted  $^{13}\text{C}(\text{g.s.})$ . Since this symmetry cannot be reached from  $^{13}\text{C}[441]$  with  $\Delta L = 0$  one understands the strong departure of  $\rho$  from the Cohen-Kurath<sup>7</sup> pickup value  $\rho \approx 1.8$ . For  $\epsilon > 0$  (weaker odd-state forces), too large a value of  $\epsilon$  would increase  $\rho$  unacceptably above the experimental value of 5 to 6, hence our choice  $\epsilon \approx 0$ .

A second point is that the lowest  $\frac{1}{2}^-$  and  $\frac{3}{2}^-$  states, mainly  $^{12}\text{C}(\text{g.s.}) \otimes (p_{1/2}, p_{3/2})_\Lambda$ , would be degenerate (Fig. 2) in the absence of  $\vec{\sigma}_\Lambda$ -core interaction. Thus independent of  $F^{(2)}$ , the small shift [Fig. 3(b)] in the "10"-MeV peak between  $0^\circ$  and

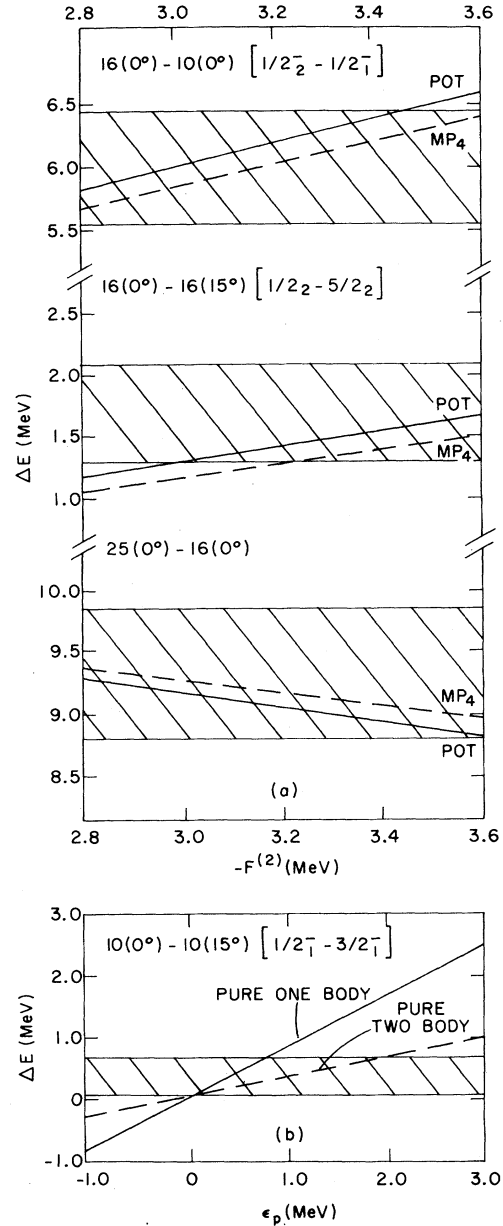


FIG. 3. Energy separations of selected pairs or groups of levels (a) as a function of  $F^{(2)}$  for  $\epsilon_p = 0.5$  MeV, (b) as a function of  $\epsilon_p$ . The strength of the pure two-body spin-orbit force is chosen to give a splitting  $\epsilon_p$  when  $p_\Lambda$  interacts with a closed  $p$  shell. The cross-hatched areas correspond to the experimentally determined separations (Ref. 1).

$15^\circ$  constrains the combination of one- and two-body spin-orbit forces to be small. Indeed, with  $\epsilon_p = 0.5$  MeV and  $v_+ = v_- = 0$ , Fig. 3 demonstrates that all measured separations can be accounted for with  $-3.4$  MeV  $< F^{(2)} < -3.0$  MeV. Specifically the  $(1.7 \pm 0.4)$ -MeV shift [Fig. 3(a)] observed<sup>1</sup> in

the "16"-MeV group in going from  $0^\circ$  to  $15^\circ$ , not particularly small relative to  $\Delta E(^{12}\text{C}; 0^+ - 2^+) = 4.43$  MeV though generated by the "weak"  $\Lambda N$  interaction, is interpreted in our calculation (Fig. 2) as due to the dominance of a  $\frac{5}{2}^-$  state at  $15^\circ$ . The separation of the "16"- and "25"-MeV peaks at  $0^\circ$  decreases as the magnitude of  $F^{(2)}$  increases [Fig. 3(a)]; indeed, in the strong-coupling limit,  $V_{\Lambda N} \simeq V_{NN}$  (implying  $|F_{\Lambda N}^{12}| \approx |F_{NN}^{(2)}| \approx 10$  MeV), all of the  $0^\circ$  strength appears, as the  $p$ -shell part of the strangeness analog state, in a single peak.

The main sensitivities in absolute cross sections due to reaction and bound-state parameters arise from uncertainties in Fermi averaging, in optical potentials obtained from preliminary examination of elastic data, and finally from uncertainties in  $\Lambda$  binding energies. Calculations throughout the  $p$  shell have been made and will be discussed in an ensuing paper. We note here, though, that the  $0^\circ$  cross section by Dover *et al.*<sup>9</sup> for  $^{12}\text{C}$  as 3.4 mb/sr for a pure  $p_{3/2}$  state bound at 1.0 MeV has been reduced to 2.0 mb/sr in much better agreement with experiment.<sup>10</sup>

A full exploitation of the structure information available from hypernuclei will require improvement in energy resolution, some of which is attainable from coincident  $\pi$ - $\gamma$  experiments, already underway. In particular the pair of  $(0p)_\Lambda$ - $(0s)_\Lambda$  E1 transitions ( $\Delta E_\gamma \simeq 10$  MeV) should in principle determine  $\epsilon_p$ . At  $\theta_\pi \simeq 0^\circ$  the  $p_{1/2}$ - $s_{1/2}$  transition is dominant and isotropic, while at  $\theta_\pi \simeq 15^\circ$  the  $p_{3/2}$ - $s_{1/2}$  correlation has the form<sup>11</sup>  $1 - 0.6 \cos^2\theta$ . Finally, the spectroscopy described here is applicable to  $\Sigma$ ,  $\Xi$ , and  $\Lambda\Lambda$  hypernuclei,

when and if these are observed in some detail.

We would like to thank B. F. Bayman for a critical reading of the manuscript and the authors of Ref. 1 for useful conversations.

This work was supported in part by the U. S. Department of Energy under Contract No. DE-AC02-76CH00016 and in part by the National Science Foundation.

<sup>(a)</sup>On leave from the Hebrew University, Jerusalem, Israel.

<sup>(b)</sup>Present address: Indiana University, Bloomington, Ind. 47405.

<sup>1</sup>M. May *et al.*, preceding Letter [Phys. Rev. Lett. **47**, 1106 (1981)].

<sup>2</sup>A. Gal, J. M. Soper, and R. H. Dalitz, Ann. Phys. (N.Y.) **113**, 79 (1978).

<sup>3</sup>The code CHUCK was used (P. D. Kunz, unpublished).

<sup>4</sup>D. R. Marlow *et al.*, Bull. Am. Phys. Soc. **25**, 724 (1980); R. A. Eisenstein, in Proceedings of the Workshop on Nuclear and Particle Physics, Los Alamos, New Mexico, 1981, Los Alamos Scientific Laboratory Report No. LA-8775-C (to be published).

<sup>5</sup>G. P. Gopal *et al.*, Nucl. Phys. **B119**, 362 (1977).

<sup>6</sup>W. Brückner *et al.*, Phys. Lett. **79B**, 157 (1978); A. Bouyssy, Phys. Lett. **91B**, 15 (1980).

<sup>7</sup>S. Cohen and D. Kurath, Nucl. Phys. **73**, 1 (1965), and **A101**, 1 (1967).

<sup>8</sup>R. H. Dalitz and A. Gal, Ann. Phys. (N.Y.) **131**, 314 (1981).

<sup>9</sup>C. B. Dover, A. Gal, G. E. Walker, and R. H. Dalitz, Phys. Lett. **89B**, 26 (1979).

<sup>10</sup>See Ref. 1; R. E. Chrien *et al.*, Phys. Lett. **89B**, 31 (1979).

<sup>11</sup>R. H. Dalitz and A. Gal, Ann. Phys. (N.Y.) **116**, 167 (1978).